Journal of Cleaner Production 292 (2021) 126050

Contents lists available at ScienceDirect

Journal of Cleaner Production

journal homepage: www.elsevier.com/locate/jclepro

The role of recycled waste glass incorporation on the carbonation behaviour of sodium carbonate activated slag mortar

G. Liu [a, b, *], M.V.A. Florea [b], H.J.H. Brouwers [b]

[a] School of Human Settlements and Civil Engineering, Xi'an Jiaotong University, Xi'an, China
[b] Department of the Built Environment, Eindhoven University of Technology, Eindhoven, the Netherlands

ARTICLE INFO

Article history:
Received 7 April 2020
Received in revised form
4 December 2020
Accepted 19 January 2021
Available online 23 January 2021

Handling editor Zhen Leng

Keywords:
Recycled waste glass
Alkali activation
Sodium carbonate
Resistance to carbonation
Performance evaluation

ABSTRACT

This study investigates the influences of recycled waste glass powder (RGP) on the carbonation behaviour of sodium carbonate activated ground granulated blast furnace slag (GGBS) mortars. The effect of activator dosages, types and RGP addition on resistance to carbonation are evaluated. The results indicate a high dosage of sodium carbonate or water glass combination as activator always can enhance the ability of resistance to carbonation. Furthermore, the addition of 30% RGP in the GGBS binder system seems to significantly improve the resistance to carbonation of mortars. The carbonation shrinkage is reduced after RGP incorporation; at the same time, a higher strength performance is observed. The RGP in sodium carbonate activated GGBS blends shows no influence on the species of reaction products. However, after carbonation, the sample containing RGP promotes the formation of nahcolite, while less bound water loss and calcium carbonate formation are identified. A high volume of gel pores (<10 nm) is formed in the RGP sample compared to specimens only containing GGBS. These properties contribute to a better resistance to carbonation for RGP containing sodium carbonate activated GGBS mortars.

1. Introduction

Cement production consumes a large quantity of energy and natural resources every year to meet the global demand for construction: 120–160 kWh of energy and 1.5 tonnes of raw materials are consumed for 1 ton of cement production (Feiz et al., 2015). In recent years, supplementary cementitious materials (SCM), such as GGBS, fly ash, silica fume and waste glass have attracted more attention as ingredients in concrete manufacture, combined with OPC (Torres-Carrasco and Puertas, 2015a; Yang et al., 2015). Most of SCMs' application still counts on the using of cement clinkers (Crossin, 2015; He et al., 2020; G. Liu et al., 2019a; Liu et al., 2018; Yang et al., 2019). In some cases, the addition of SCMs can reduce the mechanical and durability performance of blended concrete because of their low reactivity (Kayali and Sharfuddin Ahmed, 2013; Zeng et al., 2012). For the high-end utilization of solid waste and resource conservation, the concept of alkali activated concrete was proposed and widely studied for decades, which has a potential to be the alternative building material to replaces ordinary cement concrete (Buchwald and Schulz, 2005; Provis, 2014).

Usually, an alkaline solution is necessary to promote the reaction of the alumina-silicate precursor of conventional alkali activated concrete. Sodium hydroxide, sodium silicate, sodium sulphate and sodium carbonate are widely used as the activator for ground granulated blast furnace slag blends (Gao et al., 2017; Yu et al., 2016; Yuan et al., 2017a). For example, GGBS can be used for providing Ca and Si in the high calcium binder system in normal alkali activated materials, the reaction product being mainly C-(A)-S-H (Brough and Atkinson, 2002). Generally, the high alkalinity of activators such as sodium hydroxide and sodium silicate can contribute to a fast reaction and high strength at early ages, however, they also may potentially cause the risks for personal safety and high costs in construction (Kovtun et al., 2015). Alternatively, sodium carbonate activated GGBS exhibits lower costs, carbon footprint and safety risk compared to sodium hydroxide and sodium silicate in various production processes (Allali et al., 2016; Yuan et al., 2017a). Comparable strength performance of sodium carbonate activated GGBS concrete and sodium hydroxide activation was reported (Kovtun et al., 2015; Yuan et al., 2017a). The main reaction products are calcite, hydrotalcite-like phases, and C-A-S-H. The reaction mechanism has been generally discussed in previous

* Corresponding author. School of Human Settlements and Civil Engineering, Xi'an Jiaotong University, Xi'an, China.
E-mail address: G.Liu@tue.nl (G. Liu).

https://doi.org/10.1016/j.jclepro.2021.126050
0959-6526/

studies (Abdalqader et al., 2019; Bernal et al., 2015; Yuan et al., 2017b).

As a silica-rich waste material, recycled waste glass (RGP) has been used as the ingredient to provide an amorphous silica source in alkali activated concrete preparation in recent years (Torres-Carrasco and Puertas, 2017; Vafaei and Allahverdi, 2017). It has been reported that the waste glass as a precursor in alkali activated GGBS blends produced C-A-S-H with a high polymerization degree (Torres-Carrasco et al., 2014), as well as a better performance compared to GGBS/fly ash mixtures (Zhang et al., 2017). During the alkali activation of waste glass, the main identified reaction product was sodium silicate gel (Torres-Carrasco and Puertas, 2015b). In addition, it was confirmed that the waste glass powder in alkali activated concrete can play a role similar to water glass in microstructure enhancement (Puertas and Torres-Carrasco, 2014). The application of waste glass aggregates in alkali activated geopolymer also was reported to exhibit the improvements of interfacial bonding with matrix (Hajimohammadi et al., 2019).

The resistance to carbonation is the most concerning property for alkali activated concrete. Due to the absence of portlandite in alkali activated systems compared to ordinary cement concrete, C-A-S-H is more prone to decalcify as the pH buffer provided by portlandite is absent (Bakharev et al., 2001), inducing a poor performance of resistance to carbonation. Many studies have investigated the mechanisms of alkali activated concrete carbonation. The proposed results indicated that the activator types and the chemical composition of binders can result in the variation of reaction products, porosity, microstructure, cracks development and strength deterioration. Consequently, the resistance to carbonation can be affected (Bernal et al., 2014; Guo and Shi, 2013). As illustrated in the previous literature, sodium carbonate activated GGBS presents the lowest resistance to carbonation compared to sodium hydroxide and sodium silicate (Bilim and Duran Atiş, 2017), which is probably induced by the low alkalinity environment. For sodium hydroxide/silicate blended activators, a high modulus of SiO_2/Na_2O was reported to present a high resistance to carbonation of alkali activated slag (Shi et al., 2018a). Similarly, in our previous investigation, superior resistance to carbonation was achieved in the waste glass containing GGBS/fly ash mortars activated by sodium carbonate/hydroxide, but the mechanism of improvement was not studied and discussed in details (G. Liu et al., 2019b). In addition, the report of durability evaluation of waste glass in sodium carbonate activated GGBS is still rare. Therefore, an overall evaluation and analysis of recycled waste glass in sodium carbonate activated GGBS and carbonation mechanism are needed, which can provide a better understanding of the role of recyeled waste glass in alkali activated systems.

The present work investigates the carbonation resistance of a neutral activator-sodium carbonate-activated GGBS/RGP mortars. The influences of activator dosage and composition on carbonation behaviour of sodium carbonate activated GGBS/RGP mortars are evaluated. The carbonation resistance of various composites containing different ratio of GGBS to RGP is tested and compared to sample activated water glass. The mechanical performance, reaction products, microstructure and shrinkage during carbonation are observed and discussed. The main objectives are to optimize the properties of alkali activated GGBS concrete and to promote the high-end utilization of recycled waste glass in construction materials.

2. Materials and methods

2.1. Characterization of raw materials

The recycled waste glass fractions (1–8 mm, mixed colour) were supplied by a glass recycling plant. Then, the RGP (recycled waste glass powder) was prepared by using a ball mill (20 min at 300 rpm). Ground granulated blast furnace slag (GGBS) was supplied by ENCI, IJmuiden, the Netherlands. The chemical compositions of RGP and GGBS were determined with X-ray fluorescence (XRF, PANalytical Epsilon 3) spectroscopy, while the specific densities were identified with Pycnometer (AccuPyc II 1340 Micromeritics). The surface areas of materials were determined by using N_2 absorption test with BET method. The loss on ignitions (at the temperature of 1000 °C) were dertermined by using oven. The related results are illustrated in Table 1. The XRD patterns of the raw materials are shown in Fig. 1. The particle size distributions were tested by using laser granulometry (Master sizer 2000) and shown in Fig. 2.

2.2. Mortar mix design

The mix design of mortars is shown in Table 2. The RGP was used to replace slag in the binder with 0%, 10%, 20% and 30% by mass. The water to binder (GGBS + RGP) ratio was 0.5 for all mixtures. Two different dosages of sodium carbonate were used in this study, with an equivalent Na_2O% of 3% and 5% of total binder mass, respectively. In addition, to study the influence of different initial extra silica source, a commercial water glass (modulus Ms = 3.3 (mass ratio of SiO_2/Na_2O) and concentration was 36.08%) was used in activator by 5% by mass of binder. Then NC5-SS with an equivalent Na_2O% of 6.16%, while NC3-SS with an equivalent Na_2O% of 4.16% by mass of binder were designed. All activators were prepared as solutions before the mixing of mortars. The mass ratio of fine aggregates (standard sand 0–2 mm) to GGBS/RGP binder was set as 3 for all mortars mixes. At the same time, paste samples were prepared according to the same procedure.

The mixing of mortars was done by using a 5-Litre Hobart mixer. At first, the dry binder and fine aggregate (standard sand) were mixed for 30 s at low speed. Then activator was added and mixed at medium speed for 120 s. Lastly, the fresh mortars were filled into the plastic mould of 40 mm × 40 mm × 160 mm and covered with plastic film until demoulding. After that, the mortar prisms were sealed by plastic film and cured for 180 days at ambient temperature (23 ± 0.5 °C) to ensure the full reaction between activator and binders. Then aged mortar and paste samples were used for further tests.

2.3. Accelerated carbonation test

Mortars after 180 days curing were moved to a carbonation chamber (AIRTEMP) with a volume of 240 L. A controlled temperature of 25 °C and atmospheric pressure were adopted. The relative humidity (RH) in the chamber was kept as 65%, and a circular flow through CO_2 gas with a concentration of 3% by volume of mixed air was applied in the chamber continuously during the test. These parameters have been widely used in previous studies for carbonation resistance evaluation (Bernal et al., 2013). The cured pastes samples were crushed into small fractions (4 mm–8 mm) for the same period (56 days) of carbonation test as mortars.

2.4. Test methods

2.4.1. Compressive strength

The compressive strengths of mortars before (after 180 days normal curing) and after 56 days accelerated carbonation were measured according to EN 196–1. The compressive strength value was calculated from the average strength of 3 prism mortar samples.

Table 1
Chemical composition and physical properties of raw materials.

Chemical composition	Recycled waste glass	Ground granulated blast furnace slag
Na_2O	14.6	/
MgO	1.3	8.6
Al_2O_3	1.9	13.2
SiO_2	68.3	29.4
SO_3	0.09	2.6
K_2O	0.70	0.4
CaO	11.9	42.7
TiO_2	0.06	1.5
Cr_2O_3	0.12	0.001
MnO	0.02	0.40
Fe_2O_3	0.36	0.37
ZnO	0.01	/
BaO	0.06	0.08
PbO	0.05	/
P_2O_5	/	/
Cl	0.02	0.01
Specific density (g/cm^3)	2.5	2.9
Specific surface area (m^2/g)	0.99	0.37
LOI	1.34	1.15

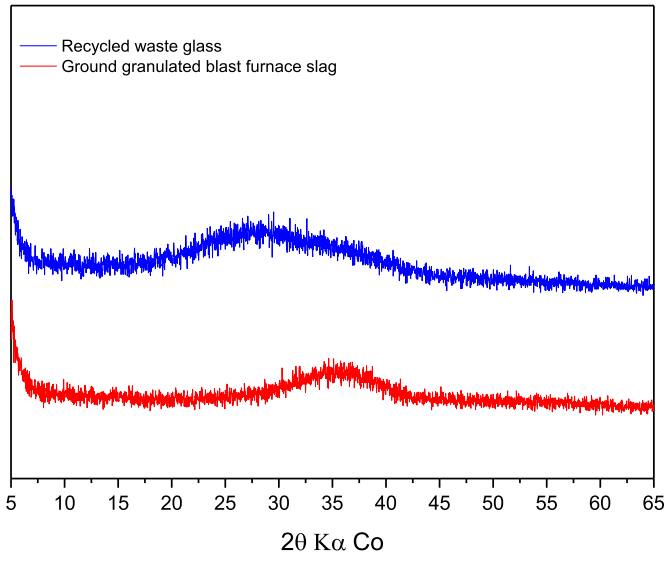

Fig. 1. XRD patterns of RGP and GGBS.

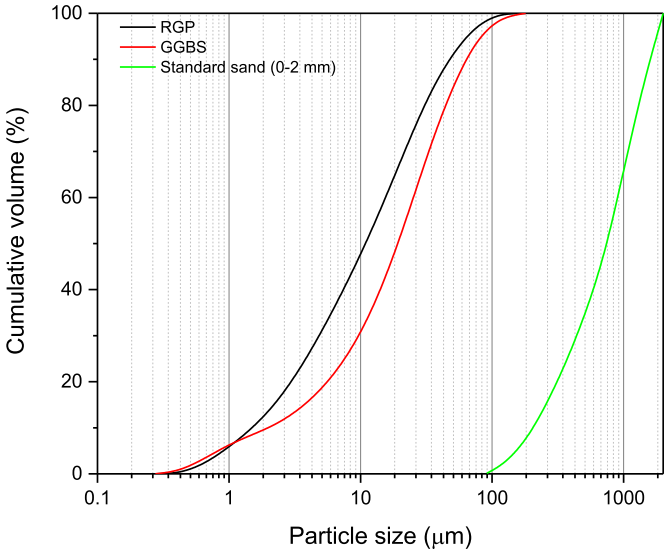

Fig. 2. Particle size distribution of materials.

2.4.2. Carbonation depth identification

A phenolphthalein solution (1% with absolute ethyl alcohol) was used to identify the carbonation depth of mortars after carbonation for 1 day, 3 days, 7 days, 14 days, 28 days, 35 days, 42 days and 56 days. Mortars were cut into two parts and then the fresh surface was sprayed with the phenolphthalein solution. To describe the carbonation depth of samples precisely, the carbonation area was determined and analysed by using Image J as shown in Fig. 3. The carbonation depth of mortars was calculated as the equation:

$$\text{Carbonation depth} = \frac{L - \sqrt{L^2 \times (A_1/A_2)}}{2} \quad (1)$$

L- side length of cross-section (40 mm)
A_1- identified area in redline (area of corss-section)
A_2- identified area in yellow line (uncarbonated area)
Then the average carbonation depth was calculated by results of three parallel mortars.

2.4.3. XRD

X-ray diffraction (Bruker D4 PHASER) with Co tube was used to study the reaction products of crushed paste samples before and after carbonation. The ball milling was used to crush pastes samples into powder for XRD. The step size was 0.018°/s, the scanning range was from 10° to 70°.

2.4.4. Thermogravimetric analysis

The thermal-gravimetric (TG) analysis of crushed paste samples before and after carbonation was conducted by using a STA 449 F1 instrument. The temperature range was set from 40 °C to 1000 °C, the heat rate was 10 °C/min and the carrier gas was N_2.

2.4.5. FTIR

The Fourier transform infrared spectroscopy (FTIR) measurement was performed in a Varian 3100 instrument with the wavenumbers ranging from 4000 to 400 cm^{-1} with a resolution of 1 cm^{-1}. The crushed paste samples before and after carbonation were tested.

2.4.6. Carbonation shrinkage

The carbonation shrinkage tests were conducted using prisms of

Table 2
Mix design of mortars (kg/m^3).

Sample	GGBS	RGP	Fine aggregates	Water	Sodium carbonate	Sodium silicate	Na_2O%
NC5	501.22	0.00	1503.65	250.61	42.85	0.00	5.00
NC5-G10	449.81	49.98	1499.36	249.89	42.72	0.00	5.00
NC5-G20	398.69	99.67	1495.09	249.18	42.60	0.00	5.00
NC5-G30	347.86	149.08	1490.85	248.47	42.48	0.00	5.00
NC5-SS	501.22	0.00	1503.65	250.61	42.85	25.06	6.16
NC3	501.22	0.00	1503.65	250.61	25.71	0.00	3.00
NC3-G10	449.81	49.98	1499.36	249.89	25.63	0.00	3.00
NC3-G20	398.69	99.67	1495.09	249.18	25.56	0.00	3.00
NC3-G30	347.86	149.08	1490.85	248.47	25.49	0.00	3.00
NC3-SS	501.22	0.00	1503.65	250.61	25.71	25.06	4.16

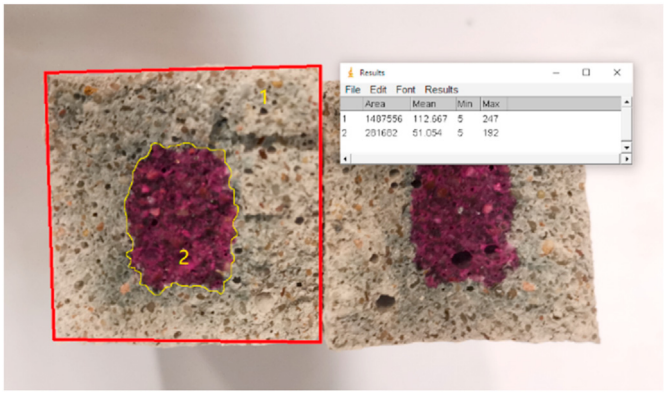

Fig. 3. The measurement of carbonation area by Image J.

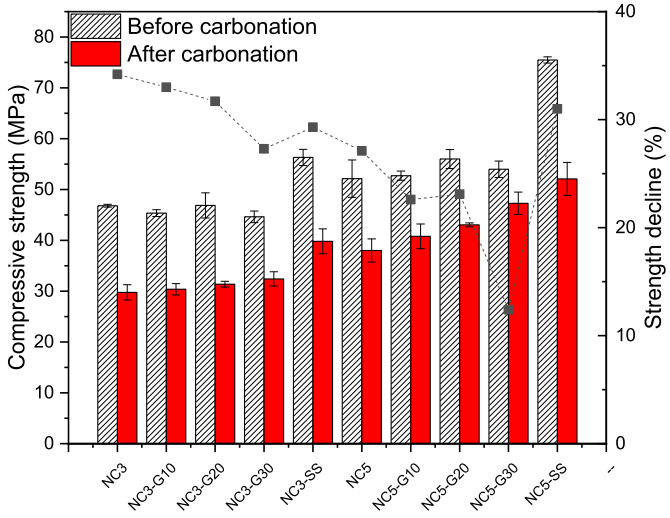

Fig. 4. The strength performance of mortars before and after carbonation.

40 mm × 40 mm × 160 mm. After 180 days of normal curing, the specimens were moved to the carbonation chamber. Then the length of different mortar samples was measured and recorded for 56 days. The carbonation shrinkage was calculated from average result of 3 parrallel mortar prisms.

2.4.7. SEM and N_2 absorption

The microstructure of samples was tested by Scanning Electron Microscopy (Phenom Pro). Nitrogen sorption analysis was conducted by TriStar II 3020, Micrometrics. The crushed paste samples before and after carbonation were tested.

3. Test results

3.1. Effect of RGP addition on strength performance after carbonation

The fact that the mechanical performance of AAS concrete can be influenced after carbonation has reported in many studies. The decalcification of C-(A)-S-H during carbonation can result in a loss of cohesion, as a consequence, a strength reduction can be observed (Bernal et al., 2010). As it can be seen in Fig. 4, the RGP addition in the binder system exhibits a slight effect on the strength performance of mortars before carbonation. The RGP blended mortars present a comparable or slightly higher strength than the reference mortar. After 56 days carbonation, all samples exhibit a variety of strength reduction. However, the NC5 series mortars still present a higher residual strength compared to mortars with NC3 series. This can be induced by the higher alkali dosage in activator which promotes the reaction degree of binder systems (Bernal, 2015), as well as a higher strength performance can be observed after alkali activation. As a consequence, a higher residual strength of carbonated mortars is presented compared to samples activated with low dosage of activator.

On the other hand, the addition of RGP ups to 30% shows no obvious strength reduction for all sodium carbonate activated mortars before carbonation. This indicates that the addition of RGP results in no negative effect on strength performance of sodium carbonate activated binder systems. Morever, it is interesting to see that the residual compressive strength keeps increasing with the RGP proportion in sodium carbonate activated mortars after 56 days carbonation. The strength decline rate keeps decreasing with the increase of RGP proportion in different mortar samples. This indicates that the addition of RGP can efficiently reduce the deterioration of strength performance of sodium carbonate activated GGBS mortars after 56 days carbonation. In the other word, the addition of RGP shows a positive effects on the resistance to carbonation of sodium carbonate activated GGBS mortars.

3.2. Effect of RGP addition on the carbonation process

3.2.1. Effect of RGP addition on carbonation depth

Fig. 5 presents the carbonation depth development of sodium activated mortars during the accelerated carbonation test. It is clearly shown that different binder systems induced the various carbonation depth at different test ages. The RGP proportion and water glass incorperation seem to show significant influences on resistance to accelerated carbonation.

It can be seen from Fig. 5 (a) that 3% Na_2O activated mortars all achieved full carbonation before the 28 days test, which achieve a carbonation depth of 20 mm. NC3 reaches the full carbonation at 20 days, however, the addition of RGP in binder system prolongs the

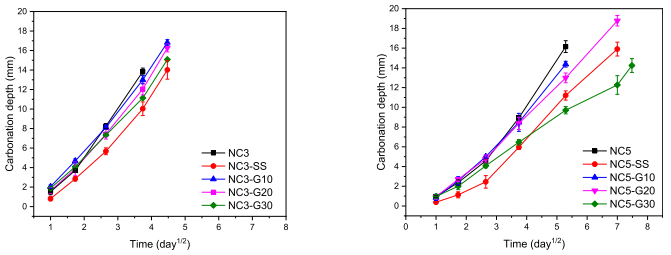

Fig. 5. Carbonation depth of different mixtures (a) 3% Na_2O% series mortars and (b) 5% Na_2O% series mortars (No data after spot means a full carbonation).

time of full carbonation to 28 days. Furthermore, the RGP blended mortars exhibit a gradually decreasing carbonation depth at 20 days with the increase of RGP proportion. The NC3-SS exhibits the best resistance to carbonation compared to other mortars, which shows the lowest carbonation depth at 20 days. On the other hand, as shown in Fig. 5 (b), a better performance of resistance to carbonation of mortars activated by a higher dosage of activator (5% of Na_2O) is observed. NC5 and NC5-G10 exhibit a full carbonation after 49 days, while NC5-G20 and NC-WG reached full carbonation after 56 days. It is noticeable that the carbonation depth of NC5-G30 is only 14 mm after 56 days, which is equal to NC5-G10 at 28 days. It is interesting to notice that NC5-G30 presents a slower carbonation depth development at a later age (after 28 days) compared to NC5-SS. However, for samples activated by low dosage of sodium carbonate, water glass activated sample (NC3-SS) still exhibit a better resistance to carbonation. This indicates that the 30% RGP addition can induce a better resistance to carbonation of higher dosage sodium carbonate activated GGBS mortars than addition of water glass. These observations indicate that, at first, the high dosage of sodium carbonate activator is beneficial to the resistance of carbonation of mortars. Secondly, the additional water glass incorporation can help to reduce the carbonation depth compared to only using sodium carbonate as activator. Lastly, the incorporation of RGP in the binder system can effectively enhance the carbonation resistance of sodium carbonate activated GGBS mortars.

It has been observed that the increase of alkali dosage and silicate modulus can effectively enhance the resistance to carbonation of alkali activated GGBS, because of the higher initial pore solution alkalinity and more activated products (Shi et al., 2018b), which agrees with the observation in the present study. However, the improvement mechanism of resistance to carbonation after RGP incorporation is rare reported. The modification mechanisms of carbonation behaviour of alkali activated materials can be caused by several factors, for example, binder system design, carbonation products, microstructure, as well as the deformation during carbonation. It has been proved that the fine glass powder as binder in alkali activated materials can release sodium and silicate in pore solution (Y. Liu et al., 2019). Then the pore solution and reaction products of alkali activated system are possible to be modified. Thus, the carbonation behaviour is expected to be changed. The detailed discussion will be addressed in the following sections.

3.2.2. Effect of RGP addition on development of carbonation shrinkage

The deformation of alkali activated materials during carbonation test can increase the risk of cracks formation, which is possible to provide more paths for CO_2 penetration. In the present study, the shrinkage of different mortars during carbonation was monitored and recorded. As it can be seen in Fig. 6, the activator dosage and the waste glass incorporation result in the different carbonation shrinkage of various specimens. For the high dosage of sodium carbonate activated samples (NC5 series), the maximum shrinkage is observed in NC5, which exhibits a total shrinkage of 7.31×10^{-4}. For low dosage sodium carbonate activated mortars, the maximum shrinkage is observed in NC3, which achieves a final carbonation shrinkage of 9.72×10^{-4}. This indicates that a high activator dosage can effectively reduce the shrinkage during carbonation because of the higher strength performance (as shown in Fig. 4) before carbonation test. Therefore, less deformation during carbonation test can be induced in high dosage activator activated samples. Samples activated by sodium carbonate/sodium silicate also present a slow shrinkage increment during the carbonation test period, which is due to the high strength performance induces a high resistance to deformation. These also contribute to better resistance to CO_2 penetration, which also agrees with the carbonation depth results in above section.

It is clear to see that the RGP addition reduces the shrinkage of all sodium carbonate activated GGBS mortars during the carbonation test period. NC3-G30 and NC5-G30 present a final carbonation shrinkage of 7.9×10^{-4} and 6.18×10^{-4}, respectively, which are reduced by 18.7% and 15.5% compared to the sample without glass powder incorporation. In addition, the waste glass incorporation contributes to a slow shrinkage increase rate. This observation corresponds with the results of carbonation depth in Section 3.2.1. On the other hand, the activator to GGBS ratio is increased after replacing by RGP, this dilution effect may increase the reaction of GGBS, which also contributes to the decreased shrinkage and increased resistance to carbonation. The correlation indicates that the fast carbonation shrinkage development induces a fast CO_2 penetration in mortars, which is reflected in a high carbonation depth. It can be concluded that the addition of RGP can effectively decrease the deformation of sodium carbonate activated GGBS mortars during carbonation, which also contributes to a better resistance to carbonation. Furthermore, normally, the carbnation process is also strongly influenced by the reaction products and microstructure change of samples after modified by RGP, which will be discussed in the following sections.

3.3. Effects of RGP addition on carbonation products

3.3.1. XRD analysis of reaction products before and after 56 days carbonation

The XRD patterns of different mixtures before and after carbonation are shown in Fig. 7. Regarding the mechanism of sodium carbonate in alkali activated slag, calcium carbonates are formatted firstly, for instance, into calcite and aragonite (Bernal et al., 2015; Kovtun et al., 2015; Yuan et al., 2017a). After the consumption of CO_3^{2-}, more OH^- is produced which increases the pH,

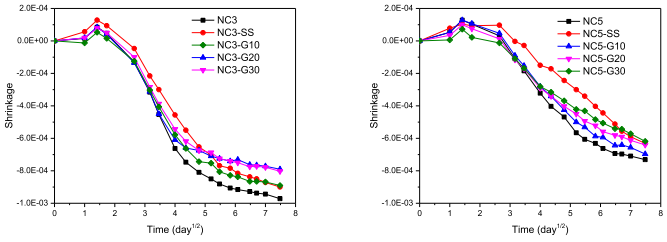

Fig. 6. Shrinkage of mortars subjected to accelerate carbonation (a) NC3 series and (b) NC5 series.

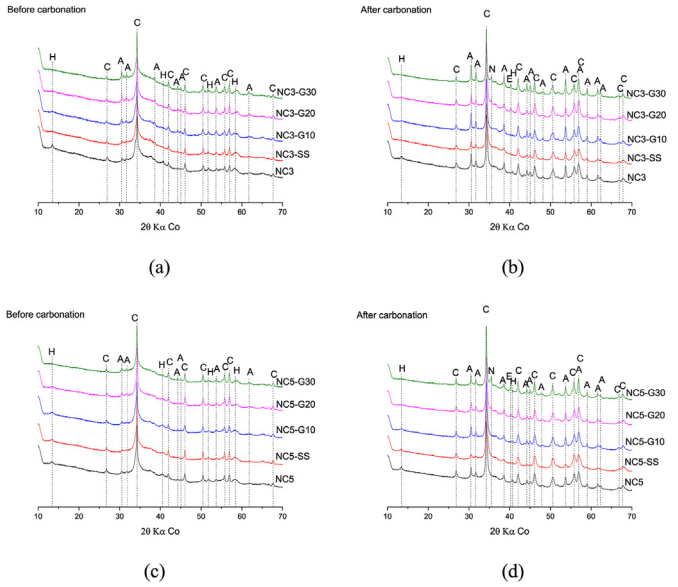

Fig. 7. XRD patterns of NC3 series samples before carbonation (a), NC3 series samples after carbonation (b), NC5 series samples before carbonation (c) and NC5 series samples after carbonation (d) (H-hydrotaclite, C- calcite, A-aragonite, N-nahcloite, E-eitelite).

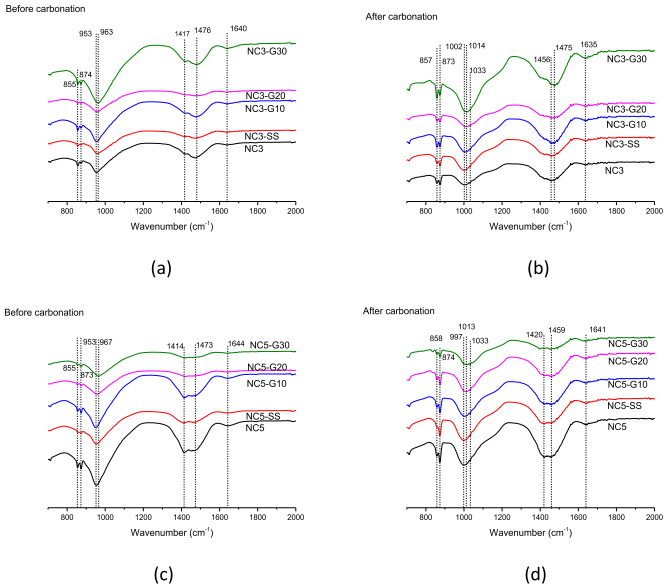

Fig. 8. FTIR of NC3 series before carbonation (a), NC5 series before carbonation (b), NC3 series after carbonation (c) and NC5 series after carbonation (d).

the slag starts reacting to form hydrotalcite and C-A-S-H. In some reports, gaylusite was also observed in only sodium carbonate or sodium carbonate-based blended activator activated slag (Chen et al., 2016; Yuan et al., 2017a). However, in the present results, there is no peak of gaylusite, which is induced by the long curing age of samples since gaylusite is not stable and will disappear at later age (Ke et al., 2016). In general, there is no difference between reaction products for samples activated by activator with various concentrations and waste glass incorporation.

However, after 56 days carbonation, new peaks are present in some samples. For sodium carbonate and sodium carbonate/water glass activated slag, the peak of hydrotalcite still exists in carbonated samples. This is induced by the stability of the LDH structure during the variation of pH (Zhi and Guo, 2005). The carbonation of C-A-S-H keeps producing calcium carbonates, which explains the sharper and more distinguished peaks of calcite and aragonite after carbonation. It is worthwhile to notice that the small addition (10%) of waste glass as binder shows a limited influence on the carbonation products. Nevertheless, when the waste glass proportion reaches 30%, significant peaks of nahcolite ($NaHCO_3$) and eitlite ($Na_2Mg(CO_3)_2$) are present in NC3-G30 and NC5-G30. This indicates that the increase of proportion of RGP in binder systems promotes the formation of nahcolite and eitlite as reaction products after carbonation compared to plain samples. Furthermore, nahcolite is a typical reaction products in alkali activated materials during carbonation, which is formed from Na present in the pore solution (Bernal et al., 2012). However, in plain samples (NC3 and NC5), there is no identifiable peaks of nahcolite can be observed, which may be caused by the low Na_2O% in the activator. This indicates that the RGP addition in binder systems can provide amount of additional Na in pore solution after reaction.

3.3.2. FTIR analysis of reaction products before and after 56 days carbonation

The FTIR results of selected samples are shown in Fig. 8. The peaks located around 874 cm^{-1} and 1417 cm^{-1} are due to the vibration of ν_3-CO_3^{2-} and ν_2-CO_3^{2-}, respectively (Yuan et al., 2017a). In addition, the peak around 874 cm^{-1} also accounts for the AlO_4^- groups in the unreacted slag particles (García-Lodeiro et al., 2008). The main peaks around 950–970 in mixtures before carbonation are assigned to the formation of C-A-S-H, which is a typical Si–O asymmetric stretching vibration generated by Q2 units (García Lodeiro et al., 2009). The peak around 1640 represents the chemical bound water (H–O–H) in hydrated mixtures.

It is noticeable that NC5-SS shows the same peak at 953 cm^{-1}, which indicates that combining sodium carbonate with water glass in activator exhibits no influences on the polymerization of Si–O for tested samples. However, a significant shift from 953 cm^{-1} to 963 cm^{-1}, and from 953 cm^{-1} to 967 cm^{-1} are observed after incorporation of RGP in binders. This reveals that the addition of waste glass in binders increases the polymerization degree of Si–O in C-A-S-H by providing more silicate, which is also observed in the previous study (G. Liu et al., 2019b). Furthermore, this observation is more significant in the NC5 series than in the NC3 series samples. The high dosage of sodium carbonate in activator is beneficial to produce more OH^-, which also promotes the reaction of waste glass particles, and then more Si can participate in the formation of C–S–H chains.

After carbonation, the peaks of Si–O in all samples shift to the higher frequency side. The bands from 997 cm^{-1} to 1014 cm^{-1} in carbonated mixtures are related to a highly polymerized Si–O in C-A-S-H gel. This is attributed to the reduced Ca ratio in C-A-S-H and the formation of amorphous silica gel during the carbonation process. This band shifting also was found in carbonated AAM activated by other kinds of activator, e.g. NaOH and Na_2SiO_3 (Shi et al., 2018b). The high polymerization of Si–O in RGP containing samples before and after carbonation indicates a relatively low Ca/Si ratio in reaction products. It has been pointed out that the C–S–H formed around the glass particles was rich in Si and Na (Mejdi et al., 2019).

3.3.3. Thermogravimetric analysis of reaction products before and after 56 days carbonation

In the case of the significantly higher carbonation resistance of sodium silicate activated samples and 30% RGP containing samples, thermogravimetric test were conducted to investigate the phase transition and evolution before and after carbonation (Fig. 9). It can

be seen that for sodium carbonate activated GGBS/RGP blends, several typical decomposition peaks are observed. The first mass loss from 100 °C to 300 °C is related to the dehydration of C-A-S-H (Burciaga-Díaz and Betancourt-Castillo, 2018). Afterwards, the mass loss between 300 and 400 °C is induced by the decomposition of hydrotalcite (Rey et al., 1992). Following the dehydration of hydrotalcite, a weak and broad peak around 600 °C is generated by the decomposition of carbonates, for example, $MgCO_3$, low crystalline calcium carbonate and amorphous calcium carbonate (Dung et al., 2019). The last small mass loss peak around 700 °C is due to the decomposition of calcite. These reaction products are also confirmed by XRD.

After carbonation, it is noticeable that the DTG curves of selected mixtures changed significantly. At first, the peaks related to C-A-S-H decomposition in carbonated mixtures all decrease. Especially for pure GGBS mortar only activated by sodium carbonate, such as NC3 and NC5. When water glass was used as activator, this was improved slightly. However, the sample containing 30% waste glass exhibits the least change in this range, which indicates that the incorporation of waste glass powder results in more residual molecular water C-A-S-H gel after carbonation. This also explains the higher strength performance of waste glass containing mortar after carbonation compared to the references. Another difference after carbonation is that the formation of the large peak around 600 °C. This change is induced by the new formation of calcium carbonates and magnesium carbonates from the decalcification of C-A-S-H during carbonation. These calcium carbonates are more related to the amorphous or low crystalline structure, which is hardly observed in XRD. In addition, the increase of these carbonates in 30% waste glass containing samples are limited compared to sodium carbonate/water glass activated mixtures. This indicates that the waste glass addition may inhibit the formation of calcium carbonates as well as enhancing the resistance to the influence of decalcification of C-A-S-H.

3.4. Effect of RGP addition on microstructure after carbonation

3.4.1. Effect of RGP modification on microstructure before and after 56 days carbonation

The microstructure images of selected paste samples before and after 56 days carbonation are shown in Fig. 10. It can be seen that the morphology of NC5 and NC5-SS exhibits a quite similar

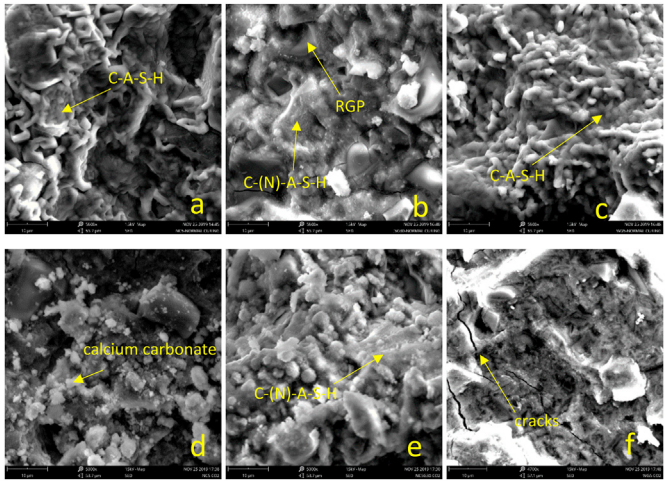

Fig. 10. SEM images of uncarbonated samples (a) NC5 (b) NC5-G30 (c) NC5-SS and (d) carbonated NC5, (e) carbonated NC5-G30, (f) carbonated NC5-SS

structure, and NC5-SS presents a more compact microstructure, which is in agreement with the above strength results (Section 3.1). However, after the incorporation of RGP, the microstructure of NC5-G30 exhibits a difference from plain GGBS samples. This may be induced by the modification of increasing RGP in the reaction products as discussed in Sections 3.3. After carbonation, a significantly loose packed particles and cracks in the sodium carbonate activated GGBS samples, and the sample activated by sodium carbonate/silicate activator can be observed. This loose structure could be caused by the decalcification of reaction products and the consequent volume change during carbonation, which is also the main reason to induce the strength reduction and carbonation shrinkage. The addition of sodium silcate increase the initial amount of SiO_2 in pore solution, which enhance the autogenous shrinkage during normal curing before carbonation test. Thus, some invisible cracks can be caused in this period, and it becomes more visible due to the decomposition of C-(A)-S-H and water evaporation after carbonation (Melo Neto et al., 2008). However, for the RGP blended sample, the microstructure of paste sample after carbonation is similar to before. This observation further confirms

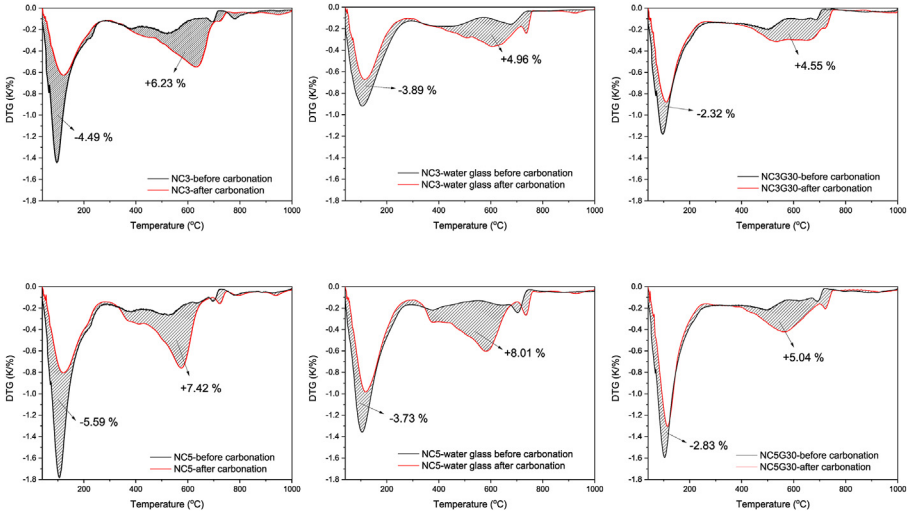

Fig. 9. DTG of samples before and after carbonation.

the limited change of microstructure in RGP blends during carbonation, and in agreement with the performance during carbonation.

3.4.2. Effect of RGP addition on gel pore structure before and after 56 days carbonation

The gel pore structures of selected mixtures tested by N_2 absorption are presented in Fig. 11. The gel microstructure of alkali activated materials can be modified during the accelerated carbonation due to the C-A-S-H decalcification and formation of carbonation products. It is clear to see that all selected mixtures exhibit a variation of gel pore volume refinement after carbonation. As illustrated in the previous discussion, the new phases formed in carbonated samples are related to calcium carbonates, for example, calcite and aragonite. These carbonation products could fill the pores and reduce the volume of larger pores in gel, or even block the pore for CO_2 transportation. Therefore, a linear relationship can be observed between carbonation depth and the square root of carbonation duration (Li et al., 2019; 2017; G. Liu et al., 2019b). This is also in agreement with the presented results in Section 3.2.1. For samples containing RGP, the peak around 20 nm significantly shifts to 10 nm, which is similar to samples which only contains GGBS. As a consequence, the pore volume less than 10 nm is enhanced obviously after carbonation for RGP blends. This indicates a strong pore modification effect in RGP blends after carbonation compared to sample only containing GGBS, which is possible due to the formation of nahcolite.

4. Discussion and conclusions

The present study investigates the carbonation behaviour after applying waste glass in sodium carbonate activated GGBS mortar.

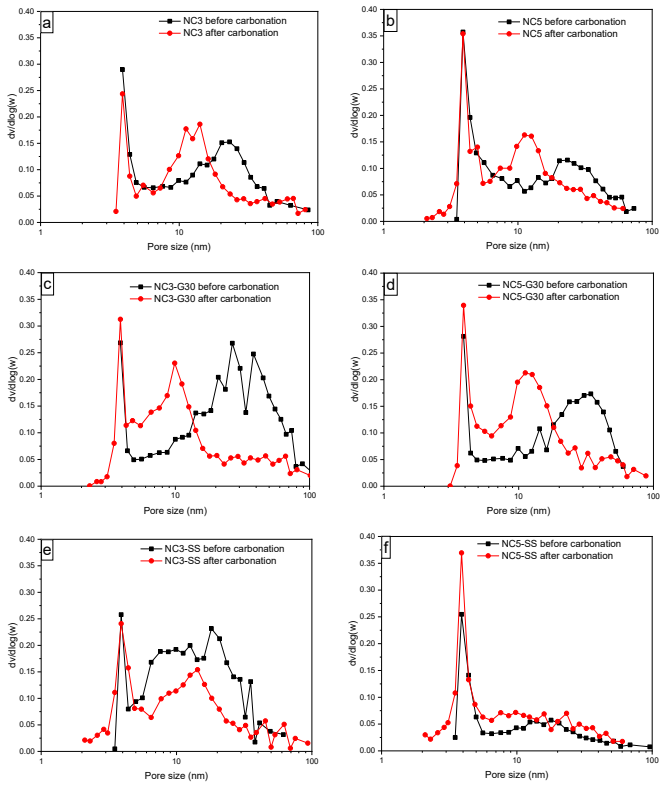

Fig. 11. Gel pore size distribution by calculation of BJH.

The influence of activator dosage and composition are investigated. The resistance to carbonation, mechanical performance, sample deformation, reaction products and microstructure variation are performed. At first, the application of RGP results in a comparable strength performance as samples containing GGBS only. This indicates that the RGP addition induces limited influence on total porosity before carbonation. In other words, the improvement of resistance to carbonation can be induced only by the variation of reaction products and modification of pore distribution after carbonation. Secondly, the incorporation of RGP does not change the reaction products species before carbonation. However, due to the reaction and disollution of RGP in alkaline environment, amount of Si can be released to form the C-(A)-S-H in alkali activated GGBS systems, which decreases the Ca/Si ratio in the reaction products. This is confirmed by the increase of polymerization of Si—O-T from FTIR results, which also agrees with the previous research (Zhang et al., 2017). In the lastest research, the low Ca/Si in C-(A)-S-H gel was observed to show a higher capacity of binding Na, which induced a lower concentration of Na in pore solution as well as a lower resistance to carbonation (Nedeljković et al., 2019). However, the addition of RGP not only shows no negative effect on the resistance to carbonation, but also reduce the deterioration during carbonation in the present study. This can be caused by the additional Na provided from the reacted RGP in alkali activated systems. It has been confirmed that the reaction of RGP in an alkaline environments can result in Na-rich C—S—H chains (Mejdi et al., 2019). Besides the Na combined by C-(A)-S-H, the Na in pore solution also could be increased after incorporation of RGP. This can be confirmed from the identifiable nacholite after carbonation test, which is related to the carbonation of Na in pore solution of alkali activated materials. Therefore, the high Na concentration from reacted RGP can result in a higher alkalinity buffer of the pore solution during carbonation. At the same time, the carbonation products in RGP blends seems to show more bound water and a lower amount of calcium carbonates from DTG results. This also confirms a higher resistance to carbonation of C-(N)-A-S-H in RGP samples. Furthermore, the nahcolite in carbonated RGP blends has a lower density (2.21 g/cm^3) than calcite and aragonite (2.71 g/cm^3). Consequently, C-(N)-A-S-H in RGP blends after carbonation exhibits better volume stability than samples only containing GGBS. This is also proved by the decrease of carbonation shrinkage as shown in Sections 3.2.2. A stronger pore refinement effect promotes the formation of more small size pores (<10 nm) in RGP blends than only GGBS samples. At a given RH, the water condensation effect occurs more easily in such a small pore or tunnel sizes. Water can easily block these small pores, and then inhibit the CO_2 transportation, which also has been found in previous studies (Nedeljković et al., 2019; Shi et al., 2018b). Therefore, less deterioration of microstructure is observed after RGP incorporation in sodium carbonate activated GGBS mortars after carbonation, as well as a higher residual strength. Based on above discussion, the following conclusions can be addressed:

1. The resistance to accelerated carbonation of sodium carbonate activated GGBS mortars are significantly improved by the incorporation of RGP, which is even better than samples activated sodium silicate. The time of full carbonation is extended to 28 days (NC3-G30) and more than 56 days (NC5-G30) from 20 days (NC3) and 28 days (NC5), respectively.
2. The incorporation of RGP ups to 30% in mortars show no obvious strength reduction before the carbonation test. After 56 days carbonation, all samples present a variety of strength reduction. However, waste glass powder containing mortars exhibit lower strength decline than reference samples.

3. The incorporation of RGP as part of binders significantly reduces the shrinkage compared to reference samples during the carbonation test, which is a possible beneficial to slow down the CO_2 penetration.
4. After carbonation, the nahcolite formation is only identified in samples containing more than 20% RGP, which may induce more clogging of pore conection compared to calcium carbonate.
5. The DTG analysis indicates that 30% of RGP incorporation reduces the bound water loss of C-A-S-H gel after carbonation. At the same time, less mass of carbonation products is observed after carbonation. This indicates that the intensity of carbonation on gel transformation was mitigated after RGP incorporation.
6. Significant refinement of capillary pore range is observed in the RGP containing samples after carbonation. The high volume of pores smaller than 10 nm is observed in RGP blends samples. These small pores may remain saturated during carbonation, which can effectively inhibit CO_2 penetration.

CRediT authorship contribution statement

G. Liu: Conceptualization, Methodology, Validation, Writing - original draft. **M.V.A. Florea:** Writing - review & editing. **H.J.H. Brouwers:** Writing - review & editing, Supervision.

Declaration of competing interest

The authors declare that they have no known competing financial interests or personal relationships that could have appeared to influence the work reported in this paper.

Acknowledgement

This research was supported by the funding of China Scholarship Council (No. 201606300062) and Eindhoven University of Technology.

References

Abdalqader, A., Jin, F., Al-Tabbaa, A., 2019. Performance of magnesia-modified sodium carbonate-activated slag/fly ash concrete. Cement Concr. Compos. 103, 160–174. https://doi.org/10.1016/j.cemconcomp.2019.05.007.

Allali, F., Joussein, E., Idrissi Kandri, N., Rossignol, S., 2016. The influence of calcium content on the mixture of sodium silicate with different additives: Na2CO3, NaOH and AlO(OH). Construct. Build. Mater. 121, 588–598. https://doi.org/10.1016/j.conbuildmat.2016.06.034.

Bakharev, T., Sanjayan, J.G., Cheng, Y.B., 2001. Resistance of alkali-activated slag concrete to carbonation. Cement Concr. Res. 31, 1277–1283. https://doi.org/10.1016/S0008-8846(01)00574-9.

Bernal, S.A., 2015. Effect of the activator dose on the compressive strength and accelerated carbonation resistance of alkali silicate-activated slag/metakaolin blended materials. Construct. Build. Mater. 98, 217–226. https://doi.org/10.1016/j.conbuildmat.2015.08.013.

Bernal, S.A., de Gutierrez, R.M., Provis, J.L., Rose, V., 2010. Effect of silicate modulus and metakaolin incorporation on the carbonation of alkali silicate-activated slags. Cement Concr. Res. 40, 898–907. https://doi.org/10.1016/j.cemconres.2010.02.003.

Bernal, S.A., Provis, J.L., Brice, D.G., Kilcullen, A., Duxson, P., Van Deventer, J.S.J., 2012. Accelerated carbonation testing of alkali-activated binders significantly underestimates service life: the role of pore solution chemistry. Cement Concr. Res. 42, 1317–1326. https://doi.org/10.1016/j.cemconres.2012.07.002.

Bernal, S.A., Provis, J.L., Myers, R.J., San Nicolas, R., van Deventer, J.S.J., 2015. Role of carbonates in the chemical evolution of sodium carbonate-activated slag binders. Mater. Struct. 48, 517–529. https://doi.org/10.1617/s11527-014-0412-6.

Bernal, S.A., Provis, J.L., Walkley, B., San Nicolas, R., Gehman, J.D., Brice, D.G., Kilcullen, A.R., Duxson, P., van Deventer, J.S.J., 2013. Gel nanostructure in alkali-activated binders based on slag and fly ash, and effects of accelerated carbonation. Cement Concr. Res. 53, 127–144. https://doi.org/10.1016/J.CEMCONRES.2013.06.007.

Bernal, S.A., San Nicolas, R., Myers, R.J., Mejía de Gutiérrez, R., Puertas, F., van Deventer, J.S.J., Provis, J.L., 2014. MgO content of slag controls phase evolution and structural changes induced by accelerated carbonation in alkali-activated binders. Cement Concr. Res. 57, 33–43. https://doi.org/10.1016/J.CEMCONRES.2013.12.003.

Bilim, C., Duran Atiş, C., 2017. Carbonation resistance OF slag mortars activated BY different alkali activators. Turkey Turkish J. Eng. 1, 1–4. https://doi.org/10.31127/tuje.315227.

Brough, A.R., Atkinson, A., 2002. Sodium silicate-based, alkali-activated slag mortars: Part I. Strength, hydration and microstructure. Cement Concr. Res. 32, 865–879. https://doi.org/10.1016/S0008-8846(02)00717-2.

Buchwald, A., Schulz, M., 2005. Alkali-activated binders by use of industrial by-products. Cement Concr. Res. 35, 968–973. https://doi.org/10.1016/j.cemconres.2004.06.019.

Burciaga-Díaz, O., Betancourt-Castillo, I., 2018. Characterization of novel blast-furnace slag cement pastes and mortars activated with a reactive mixture of MgO-NaOH. Cement Concr. Res. 105, 54–63. https://doi.org/10.1016/j.cemconres.2018.01.002.

Chen, Y., Shui, Z., Chen, W., Li, Q., Chen, G., 2016. Effect of MgO content of synthetic slag on the formation of Mg-Al LDHs and sulfate resistance of slag-fly ash-clinker binder. Construct. Build. Mater. 125, 766–774. https://doi.org/10.1016/j.conbuildmat.2016.08.086.

Crossin, E., 2015. The greenhouse gas implications of using ground granulated blast furnace slag as a cement substitute. J. Clean. Prod. 95, 101–108. https://doi.org/10.1016/J.JCLEPRO.2015.02.082.

Dung, N.T., Hooper, T.J.N., Unluer, C., 2019. Accelerating the reaction kinetics and improving the performance of Na2CO3-activated GGBS mixes. Cement Concr. Res. 126, 105927 https://doi.org/10.1016/j.cemconres.2019.105927.

Feiz, R., Ammenberg, J., Eklund, M., Helgstrand, A., Marshall, R., 2015. Improving the CO2 performance of cement, part I: utilizing life-cycle assessment and key performance indicators to assess development within the cement industry. J. Clean. Prod. 98, 272–281. https://doi.org/10.1016/J.JCLEPRO.2014.01.083.

Gao, X., Yu, Q.L., Lazaro, A., Brouwers, H.J.H., 2017. Investigation on a green olivine nano-silica source based activator in alkali activated slag-fly ash blends: reaction kinetics, gel structure and carbon footprint. Cement Concr. Res. 100, 129–139. https://doi.org/10.1016/j.cemconres.2017.06.007.

García-Lodeiro, I., Fernández-Jiménez, A., Blanco, M.T., Palomo, A., 2008. FTIR study of the sol-gel synthesis of cementitious gels: C-S-H and N-A-S-H. J. Sol. Gel Sci. Technol. 45, 63–72. https://doi.org/10.1007/s10971-007-1643-6.

García Lodeiro, I., Macphee, D.E., Palomo, A., Fernández-Jiménez, A., 2009. Effect of alkalis on fresh C-S-H gels. FTIR analysis. Cement Concr. Res. 39, 147–153. https://doi.org/10.1016/j.cemconres.2009.01.003.

Guo, X., Shi, H., 2013. Modification of steel slag powder by mineral admixture and chemical activators to utilize in cement-based materials. Mater. Struct. 46, 1265–1273. https://doi.org/10.1617/s11527-012-9970-7.

Hajimohammadi, A., Ngo, T., Vongsvivut, J., 2019. Interfacial chemistry of a fly ash geopolymer and aggregates. J. Clean. Prod. 231, 980–989. https://doi.org/10.1016/j.jclepro.2019.05.249.

He, X., Zheng, Z., Yang, J., Su, Y., Wang, T., Strnadel, B., 2020. Feasibility of incorporating autoclaved aerated concrete waste for cement replacement in sustainable building materials. J. Clean. Prod. 250, 119455 https://doi.org/10.1016/j.jclepro.2019.119455.

Kayali, O., Sharfuddin Ahmed, M., 2013. Assessment of high volume replacement fly ash concrete – concept of performance index. Construct. Build. Mater. 39, 71–76. https://doi.org/10.1016/J.CONBUILDMAT.2012.05.009.

Ke, X., Bernal, S.A., Provis, J.L., 2016. Controlling the reaction kinetics of sodium carbonate-activated slag cements using calcined layered double hydroxides. Cement Concr. Res. 81, 24–37. https://doi.org/10.1016/j.cemconres.2015.11.012.

Kovtun, M., Kearsley, E.P., Shekhovtsova, J., 2015. Chemical acceleration of a neutral granulated blast-furnace slag activated by sodium carbonate. Cement Concr. Res. 72, 1–9. https://doi.org/10.1016/j.cemconres.2015.02.014.

Li, N., Farzadnia, N., Shi, C., 2017. Microstructural changes in alkali-activated slag mortars induced by accelerated carbonation. Cement Concr. Res. 100, 214–226. https://doi.org/10.1016/j.cemconres.2017.07.008.

Li, N., Shi, C., Zhang, Z., 2019. Understanding the roles of activators towards setting and hardening control of alkali-activated slag cement. Compos. B Eng. 171, 34–45. https://doi.org/10.1016/j.compositesb.2019.04.024.

Liu, G., Florea, M.V.A., Brouwers, H.J.H., 2019a. Performance evaluation of sustainable high strength mortars incorporating high volume waste glass as binder. Construct. Build. Mater. 202, 574–588. https://doi.org/10.1016/J.CONBUILDMAT.2018.12.110.

Liu, G., Florea, M.V.A., Brouwers, H.J.H., 2019b. Waste glass as binder in alkali activated slag–fly ash mortars. Mater. Struct. Constr. 52 https://doi.org/10.1617/s11527-019-1404-3.

Liu, G., Florea, M.V.A., Brouwers, H.J.H., 2018. The hydration and microstructure characteristics of cement pastes with high volume organic-contaminated waste glass powder. Construct. Build. Mater. 187, 1177–1189. https://doi.org/10.1016/J.CONBUILDMAT.2018.07.162.

Liu, Y., Shi, C., Zhang, Z., Li, N., 2019. An overview on the reuse of waste glasses in alkali-activated materials. Resour. Conserv. Recycl. https://doi.org/10.1016/j.resconrec.2019.02.007.

Mejdi, M., Wilson, W., Saillio, M., Chaussadent, T., Divet, L., Tagnit-Hamou, A., 2019. Investigating the pozzolanic reaction of post-consumption glass powder and the role of portlandite in the formation of sodium-rich C-S-H. Cement Concr. Res. 123, 105790 https://doi.org/10.1016/j.cemconres.2019.105790.

Melo Neto, A.A., Cincotto, M.A., Repette, W., 2008. Drying and autogenous shrinkage of pastes and mortars with activated slag cement. Cement Concr. Res. 38,

565–574. https://doi.org/10.1016/j.cemconres.2007.11.002.
Nedeljković, M., Ghiassi, B., van der Laan, S., Li, Z., Ye, G., 2019. Effect of curing conditions on the pore solution and carbonation resistance of alkali-activated fly ash and slag pastes. Cement Concr. Res. 116, 146–158. https://doi.org/10.1016/j.cemconres.2018.11.011.
Provis, J.L., 2014. Geopolymers and other alkali activated materials: why, how, and what? Mater. Struct. Constr. 47, 11–25. https://doi.org/10.1617/s11527-013-0211-5.
Puertas, F., Torres-Carrasco, M., 2014. Use of glass waste as an activator in the preparation of alkali-activated slag. Mechanical strength and paste characterisation. Cement Concr. Res. 57, 95–104. https://doi.org/10.1016/J.CEMCONRES.2013.12.005.
Rey, F., Fornés, V., Rojo, J.M., 1992. Thermal decomposition of hydrotalcites. An infrared and nuclear magnetic resonance spectroscopic study. J. Chem. Soc., Faraday Trans. 88, 2233–2238. https://doi.org/10.1039/FT9928802233.
Shi, Z., Shi, C., Wan, S., Li, N., Zhang, Z., 2018a. Effect of alkali dosage and silicate modulus on carbonation of alkali-activated slag mortars. Cement Concr. Res. 113, 55–64. https://doi.org/10.1016/J.CEMCONRES.2018.07.005.
Shi, Z., Shi, C., Wan, S., Li, N., Zhang, Z., 2018b. Effect of alkali dosage and silicate modulus on carbonation of alkali-activated slag mortars. Cement Concr. Res. https://doi.org/10.1016/J.CEMCONRES.2018.07.005.
Torres-Carrasco, M., Palomo, J.G., Puertas, F., 2014. Sodium silicate solutions from dissolution of glasswastes. Statistical analysis. Mater. Constr. 64 https://doi.org/10.3989/mc.2014.05213.
Torres-Carrasco, M., Puertas, F., 2017. Waste glass as a precursor in alkaline activation: chemical process and hydration products. Construct. Build. Mater. 139, 342–354. https://doi.org/10.1016/J.CONBUILDMAT.2017.02.071.
Torres-Carrasco, M., Puertas, F., 2015a. Waste glass in the geopolymer preparation. Mechanical and microstructural characterisation. J. Clean. Prod. 90, 397–408. https://doi.org/10.1016/J.JCLEPRO.2014.11.074.
Torres-Carrasco, M., Puertas, F., 2015b. Waste glass in the geopolymer preparation. Mechanical and microstructural characterisation. J. Clean. Prod. 90, 397–408. https://doi.org/10.1016/j.jclepro.2014.11.074.
Vafaei, M., Allahverdi, A., 2017. High strength geopolymer binder based on waste-glass powder. Adv. Powder Technol. 28, 215–222. https://doi.org/10.1016/J.APT.2016.09.034.
Yang, J., Huang, J., Su, Y., He, X., Tan, H., Yang, W., Strnadel, B., 2019. Eco-friendly treatment of low-calcium coal fly ash for high pozzolanic reactivity: a step towards waste utilization in sustainable building material. J. Clean. Prod. 238, 117962 https://doi.org/10.1016/j.jclepro.2019.117962.
Yang, K.-H., Jung, Y.-B., Cho, M.-S., Tae, S.-H., 2015. Effect of supplementary cementitious materials on reduction of CO2 emissions from concrete. J. Clean. Prod. 103, 774–783. https://doi.org/10.1016/J.JCLEPRO.2014.03.018.
Yu, B.-W., Du, Y.-J., Jin, F., Liu, C.-Y., 2016. Multiscale study of sodium sulfate soaking durability of low plastic clay stabilized by reactive magnesia-activated ground granulated blast-furnace slag. J. Mater. Civ. Eng. 28, 04016016 https://doi.org/10.1061/(ASCE)MT.1943-5533.0001517.
Yuan, B., Yu, Q.L., Brouwers, H.J.H., 2017a. Time-dependent characterization of Na 2 CO 3 activated slag. Cement Concr. Compos. 84, 188–197. https://doi.org/10.1016/j.cemconcomp.2017.09.005.
Yuan, B., Yu, Q.L., Brouwers, H.J.H., 2017b. Assessing the chemical involvement of limestone powder in sodium carbonate activated slag. Mater. Struct. 50, 136. https://doi.org/10.1617/s11527-017-1003-0.
Zeng, Q., Li, K., Fen-chong, T., Dangla, P., 2012. Pore structure characterization of cement pastes blended with high-volume fly-ash. Cement Concr. Res. 42, 194–204. https://doi.org/10.1016/J.CEMCONRES.2011.09.012.
Zhang, S., Keulen, A., Arbi, K., Ye, G., 2017. Waste glass as partial mineral precursor in alkali-activated slag/fly ash system. Cement Concr. Res. 102, 29–40. https://doi.org/10.1016/j.cemconres.2017.08.012.
Zhi, P.X., Guo, Q.L., 2005. Hydrothermal synthesis of layered double hydroxides (LDHs) from mixed MgO and Al2O3: LDH formation mechanism. Chem. Mater. 17, 1055–1062. https://doi.org/10.1021/cm048085g.